Mechanical Slosh Models for Rocket-Propelled Spacecraft

Jiann-Woei Jang[1], Abran Alaniz[2], and Lee Yang[3]
The Charles Stark Draper Laboratory, Inc., Houston, TX, 77058

and

Joseph Powers[4], and Charles Hall[5]
NASA/George C. Marshall Space Flight Center, Huntsville, AL, 35812

Several analytical mechanical slosh models for a cylindrical tank with flat bottom are reviewed. Even though spacecrafts use cylinder shaped tanks, most of those tanks usually have elliptical domes. To extend the application of the analytical models for a cylindrical tank with elliptical domes, the modified slosh parameter models are proposed in this report by mapping an elliptical dome cylindrical tank to a flat top/bottom cylindrical tank while maintaining the equivalent liquid volume. For the low Bond number case, the low-g slosh models were also studied. Those low-g models can be used for Bond number > 10. The current low-g slosh models were also modified to extend their applications for the case that liquid height is smaller than the tank radius. All modified slosh models are implemented in MATLAB m-functions and are collected in the developed MST (Mechanical Slosh Toolbox).

Nomenclature

R_0: tank radius
h: liquid height
m_n: the n^{th} slosh mass
w_n: the n^{th} slosh mode frequency
ζ_n: the n^{th} slosh mode damping
h_n: the n^{th} slosh mass location from liquid level
l_n: equivalent pendulum length for n^{th} slosh mass
Z_n: the n^{th} slosh mass displacement
f_{rs}: the coupling force between rigid and slosh dynamics
f_{fs}: the coupling force between flex and slosh dynamics
V: characteristic velocity
ρ: liquid density
σ: liquid surface tension
We: Weber number
Bo: Bond number
Ga: Galileo number

[1]Principal Member of the Technical Staff; Draper Laboratory, Houston, TX, 77058: jang@draper.com, AIAA Senior Member
[2]Member of the Technical Staff; Draper Laboratory, Houston, TX, 77058: aalaniz@draper.com
[3]Senior Member of the Technical Staff; Draper Laboratory, Cambridge, MA, 02139: lyang@draper.com
[4]Senior Aerospace Engineer; NASA Marshall Space Flight Center, Huntsville, AL 35812:Joseph.F.Powers@nasa.gov
[5]Senior Aerospace Engineer; NASA Marshall Space Flight Center, Huntsville, AL 35812: Charles.E.Hall@nasa.gov

a: vehicle axial acceleration
ϕ: velocity potential
r, θ, z: axes of tank-fixed coordinate system in Figure 3
λ_m: m^{th} zeros of the derivative of the Bessel Function of the 1^{st} kind, J_1
t: time
p: fluid pressure
v: fluid velocity
m_{liq}: liquid mass
k_v: kinematic viscosity of the liquid.
d: dome depth
l: total tank length
R_0^*: equivalent tank radius with dome correction
h^*: equivalent liquid height with dome correction
η: wave height above meniscus as shown in Figure 3
ε: nondimensional wave height above meniscus ($\varepsilon = \eta / R_0$)
β: nondimensional meniscus height at tank wall
a_n: expansion coefficient in series for ϕ
b_n: expansion coefficient in series for ε
$C1_{mn}$, $C2_{mn}$, $C3_{mn}$: Fourier-Bessel coefficients
Ω_n: dimensionless natural frequency of n^{th} slosh mass

I. Introduction

When modeling the dynamics for a rocket-propelled spacecraft, it is very important to properly predict the behavior of liquid in a propellant tank. There are two approaches to model the liquid sloshing dynamics. One uses CFD (Computational Fluid Dynamics) theory, while the other approximates the liquid behavior using a spring-mass-damper mechanical model. The former approach is usually used to predict slosh mass motion in time-domain simulation. The latter is used in the frequency domain analysis to predict the interaction between slosh and other space vehicle dynamics. In this research, several mechanical slosh models ([1] to [4]) are reviewed. The high-g slosh parameter model [1] has been derived for a cylindrical tank with a flat top and bottom. Even though spacecraft use cylinder shaped tanks, most of those tanks usually have elliptical domes. To extend the application of the analytical model in [1] for a cylindrical tank with elliptical domes, modified high-g slosh parameter models are proposed in this report by mapping a elliptical dome cylindrical tank to a flat top/bottom cylindrical tank while maintaining the equivalent liquid volume. Several analytical low-g slosh parameter models ([2] to [4]) are also studied in this research. Under the assumption that the liquid height is larger than the radius of the tank, those low-g models ([2] to [4]) were derived for a flat bottom shaped cylindrical tank. In this research, those low-g parameter models are modified to extend their application for the case that the liquid height in the tank is smaller than the radius of the tank. The same technique which extends the application of the high-g slosh parameters model to account for the dome area can be applied to the modified low-g models. The contents of the report are outlined as follows. First, the high-g slosh parameters model is briefly reviewed. The modified high-g slosh parameters model is derived next. The low-g models for a cylindrical tank with a flat top and bottom will also be reviewed. The necessary modification which extends the application of the reviewed low-g models is also introduced. One modification is for the case that liquid height is less than the radius of the tanks while the other one is for the tanks with elliptical domes. All

modified high-g and low-g slosh models are implemented in MATLAB m-functions and are collected in the developed MST (Mechanical Slosh Toolbox). A brief summary of the code flows in terms of the equations to get to the slosh parameters are also provided in this report. The outputs of MST are the slosh parameters, which include slosh frequency, slosh mass, slosh location and smooth wall slosh damping, as functions of the liquid level in the corresponding mechanical slosh model.

II. Mechanical Slosh Models

The main interest of the slosh dynamics is the lateral sloshing motion or oscillation of the liquid mass. The mechanical slosh model approximates the motion of the movable liquid mass with a rigid mass plus a mass-spring-damper model [1] (Figure 1).

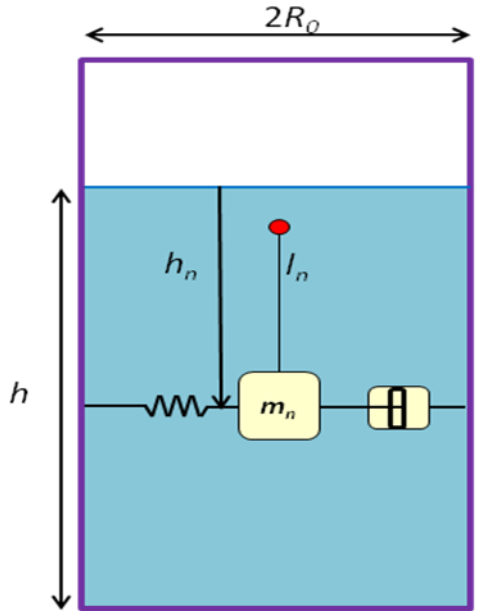

Figure 1. Mechanical Models of Sloshing for a Cylindrical Tank

The corresponding Laplace transformed mechanical slosh model can be mathematically formulated as [5]

$$m_n(s^2 + 2\zeta_n w_n s + w_n^2)Z_n = f_{rs} + f_{fs} \tag{1}$$

The slosh mass, frequency, damping and location in the above equation are functions of physical properties of the liquid, liquid level, the tank radius, and the axial body force acting upon the space vehicle.

III. Hydrodynamic Regimes

The motion of liquid mass was driven by the resultants of the capillary force, body force, inertia force and viscous force. The relativity of each force to the others determines the hydrodynamic region [1]. As shown in Figure 2, the relative importance of inertia and capillary force is defined as Weber number, i.e.

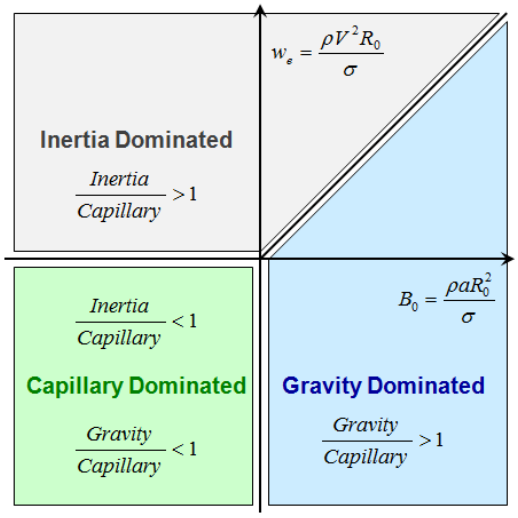

Figure 2. Hydrodynamic Regimes [1]

$$We = \frac{Inertia}{Capillary} = \frac{\rho V^2 R_0}{\sigma} \tag{2}$$

Similarly, the acceleration to capillary forces ratio is defined as Bond number, i.e.,

$$Bo = \frac{Acceleration}{Capillary} = \frac{\rho a R_0^2}{\sigma} \tag{3}$$

The dimensionless Bond number will determine the shape of the equilibrium surface of the liquid tank as shown in Figure 3 [3]. For Bond number ≥ 1000, the equilibrium liquid surface is reasonably flat. This scenario is classified as a high-g slosh problem. The contact angle is defined as the angle between the water line and the wall. In a high-g problem, the contact angle is equal to 90 degrees. As the Bond number decreases, the equilibrium interface starts curving. When the Bond number approaches 0, the water line will be parallel to the wall, thus the corresponding contact angle is equal to 0 degrees.

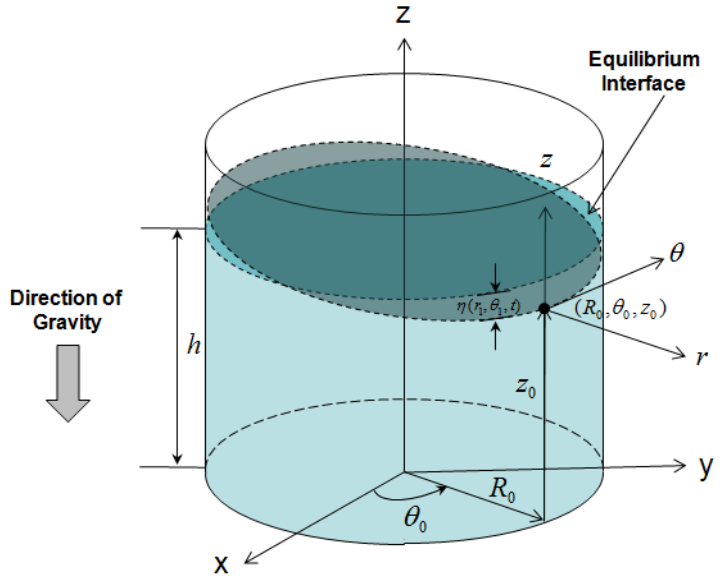

Figure 3. Equilibrium of Liquid Surface

IV. High-G Slosh Parameter [1]

For an incompressible flow, the velocity potential $\phi(r,\theta,z)$ must satisfy Laplace's equation everywhere in the liquid volume, i.e.

$$\nabla^2\phi = 0 \tag{4}$$

and two boundary conditions

$$\left.\frac{\partial\phi}{\partial r}\right|_{r=R_0} = 0 \tag{5}$$

$$\left.\frac{\partial\phi}{\partial z}\right|_{z=-h} = 0 \tag{6}$$

The steady state solution to the above Laplace equation satisfying those boundary conditions is

$$\phi(r,\theta,z) = \sum_{m,n} A_{mn} J_n(\lambda_m \frac{r}{R_0})\cos(n\theta)\frac{\cosh(\lambda_m \frac{z+h}{R_0})}{\cosh(\lambda_m \frac{h}{R_0})} \tag{7}$$

where the values of coefficients A_{mn} can be solved for a given set of boundary conditions. For an irrotational flow, the slosh liquid motion can be described by the unsteady form of Bernoulli's equation

$$\frac{\partial\Phi(r,\theta,z,t)}{\partial t} + az(r,\theta,t) + \frac{v^2}{2} + \frac{p}{\rho} = 0 \tag{8}$$

The corresponding time-dependent solution is

$$\Phi(r,\theta,z,t) = \phi(r,\theta,z)e^{iwt} \tag{9}$$

Linearizing the unsteady form of Bernoulli's equation at the free surface and applying the following "Kinematic" condition

$$\frac{\partial\delta}{\partial t} = w = \frac{\partial\Phi}{\partial z} \quad for \qquad z = \frac{h}{2} \tag{10}$$

the time derivative of the linearized Bernoulli's equation becomes

$$\frac{\partial^2\Phi}{\partial t^2} + a\frac{\partial\Phi}{\partial z} = 0 \qquad for \qquad z = \frac{h}{2} \tag{11}$$

Plug Eq.(9) into the above equation and solve for w_n

$$w_n^2 = \lambda_m \frac{a}{R_0}\tanh(\lambda_m \frac{h}{R_0}) \tag{12}$$

The corresponding slosh location (h_n) measured from liquid level and slosh mass (m_n) can be derived as [1]

$$m_n = m_{liq}\frac{2R_0\tanh\left(\lambda_n\frac{h}{R_0}\right)}{\lambda_n h\left(\lambda_n^2 - 1\right)} \tag{13}$$

$$h_n = \frac{2R_0}{\lambda_n}\tanh\left(\lambda_n\frac{h}{2R_0}\right) \tag{14}$$

The slosh damping due to the physical baffles installed inside the tank can be estimated by using the energy dissipation rate of a force free oscillation. For oscillation, the slosh damping can be approximated with [6]

$$\zeta = \frac{\Delta}{\sqrt{4\pi^2 + \Delta^2}} \tag{15}$$

where Δ is defined as the logarithmic decrement

$$\Delta = \ln\left(\frac{\text{Current Peak Response}}{\text{Next Peak Response}}\right) \tag{16}$$

Eq. (15) is usually used to interpret experimental measurement. The analytical slosh damping formulas for anti-slosh devices are available in [1] based on fluid dynamics analysis. Liquid slosh in a cylindrical tank without an anti-slosh device is damped by the viscous stresses. This type of damping is labeled as the smooth wall damping. The model of the smooth wall damping of the 1st slosh mass for a circular cylindrical tank has been derived [1]

$$h \le R_0 \qquad \zeta_1 = 0.79\sqrt{Re}\left[1 + \frac{0.318}{\sinh\left(1.84\frac{h}{R_0}\right)}\left(1 + \frac{1-\frac{h}{R_0}}{\cosh\left(1.84\frac{h}{R_0}\right)}\right)\right] \tag{17}$$

$$h > R_0 \qquad \zeta_1 = 0.79\sqrt{Re}$$

where the dimensionless parameter *Re* is defined as

$$Re = \frac{k_v}{\sqrt{aR_0^3}} \tag{18}$$

The mechanical slosh parameter models cited in the section are valid if slosh displacements are small. If the wave amplitude due to the axial load is greater than 10% of the tank diameter, splashing, breaking waves and even rotary sloshing will occur, thus the apparent slosh damping will increase in the mechanical slosh model [1].

V. High-G Slosh Parameters for a Cylindrical Tank with Elliptical Domes

The slosh models cited in the previous section are derived for a cylindrical tank with a flat bottom as shown in Figure 1. Most propellant tanks in a space vehicle have both elliptical top and bottom domes as shown in Figure 4. The slosh parameter models for a flat bottom cylindrical tank cannot be directly applied to the dome area. One way to resolve this issue is to map a cylindrical tank with top and bottom dome to a cylindrical tank with flat top and bottom while maintaining the equivalent liquid volume [7]. Given a tank radius of R_0, a dome depth of d and a total tank length of l, the formula for the dome area correction follows.

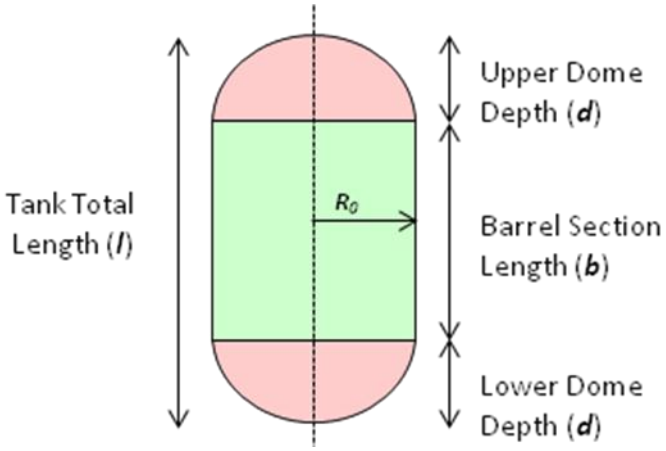

Figure 4. Cylindrical Tank with Elliptical Domes

For the case of liquid level in the top dome area, the equivalent tank radius (R_0^*) and liquid height (h^*) for a cylindrical tank with flat top and bottom can be derived as

$$R_0^* = R_0\sqrt{\frac{(l-h)(2d+h-l)}{d^2}}$$
$$h^* = \frac{2d^3 - 3ld^2 + (3h^2 - 6hl + 3l^2)d + h^3 - 3h^2l + 3hl^2 - l^3}{(6h-6l)d + 3h^2 - 6hl + 3l^2} \tag{19}$$

When the liquid level is in the barrel section as shown in Figure 5, the equivalent tank radius (R_0^*) and liquid height (h^*) for a cylindrical tank with flat top and bottoms can be derived as

$$R_0^* = R_0$$
$$h^* = h - \frac{d}{3} \tag{20}$$

For the case of the liquid level in the bottom dome area, the equivalent tank radius (R_0^*) and liquid height (h^*) for a cylindrical tank with a flat bottom can be derived as

$$R_0^* = R_0\sqrt{\frac{h(2d-h)}{d^2}}$$
$$h^* = \frac{h(3d-h)}{6d-3h} \tag{21}$$

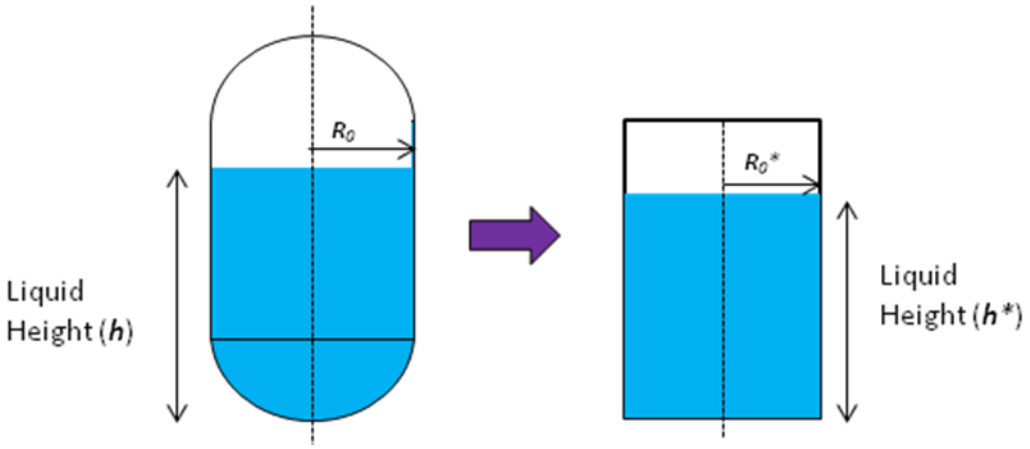

Figure 5. Slosh Parameter Correction for a Cylindrical Tank with Elliptical Domes

VI. Low-g Slosh Parameters for a Cylindrical Tank

Equation (7) in the high-g parameter section can be made nondimensional by replacing r/R_0 with R and setting n = 1 ([2]-[4]).

$$\phi(R,\theta,Z,\tau) = \sum_{m=1}^{\infty} a_m(\tau) J_1(\lambda_m R)\cos(\theta) e^{\lambda_m Z} \tag{22}$$

The nondimensional wave shape ($\varepsilon = \eta / R_0$) can be modeled as [3]

$$\varepsilon(R,\theta,\tau) = \sum_{m=1}^{\infty} b_m(\tau) J_1(\lambda_m R)\cos(\theta) \tag{23}$$

where η is the wave height above meniscus as shown in Figure 3. Based on the boundary conditions, the motion of the free surface and the fluid velocity at the free surface must be equal to each other, i.e.

$$\frac{\partial \varepsilon}{\partial \tau} - \frac{\partial \phi}{\partial Z} + \frac{dF}{dR}\left(\frac{\partial \phi}{\partial R}\right) = 0, \qquad Z = F \tag{24}$$

$$\frac{\partial \phi}{\partial \tau} + \varepsilon - \frac{1}{N_{BO}}\left(\frac{1}{R}\frac{\partial}{\partial R}\left\{\frac{R\dfrac{\partial \varepsilon}{\partial R}}{\left(1+\left(\dfrac{dF}{dR}\right)^2\right)^{3/2}}\right\} + \frac{1}{R^2}\frac{\partial}{\partial \theta}\left\{\frac{\dfrac{\partial \varepsilon}{\partial \theta}}{\left(1+\left(\dfrac{dF}{dR}\right)^2\right)^{1/2}}\right\}\right) - X_0\Omega^2 R\cos\theta\sin\Omega t = 0, \qquad Z = F \tag{25}$$

where

$$F = \beta\left[1-\left(1-\frac{r^3}{R_0^3}\right)^{1/2}\right] \tag{26}$$

β is the largest positive root of the following polynomial

$$\beta^3 N_{BO} - \beta^2 - 2/3 = 0 \tag{27}$$

Solve the two boundary conditions (Equations (24) and (25))

$$\sum_{n=1}^{\infty}\left\{\dot{b}_n + \sum_{m=1}^{\infty} C1_{mn}\, a_m\right\} J_1(\lambda_n R)\cos\theta = 0 \tag{28}$$

$$\sum_{n=1}^{\infty}\left\{b_n + \sum_{m=1}^{\infty} C2_{mn}\,\dot{a}_m + \sum_{m=1}^{\infty} C3_{mn}\, b_m - \frac{2X_0\Omega^2}{\left(\lambda_n^2-1\right)J_1(\lambda_n)}\sin\Omega t\right\} J_1(\lambda_n R)\cos\theta = 0 \tag{29}$$

and combine the above two equations by eliminating b_n

$$\sum_{m=1}^{\infty} C2_{mn}\,\ddot{a}_m - \sum_{m=1}^{\infty} C1_{mn}\, a_m - \sum_{s=1}^{\infty}\left(C3_{mn}\sum_{m=1}^{\infty} C1_{sm}\, a_m\right) = \frac{2X_0\Omega^3}{\left(\lambda_n^2-1\right)J_1(\lambda_n)}\cos\Omega t \tag{30}$$

where

$$\begin{aligned}
C1_{mn} &= \frac{2\lambda_n^2}{\left(\lambda_n^2-1\right)\left(J_1(\lambda_n)\right)^2}\int_0^1 R\left\{-\lambda_m J_1(\lambda_m R) + \frac{3\beta R^2}{2\left(1-R^3\right)^{1/2}} J_1'(\lambda_m R)\right\} \\
&\qquad \times J_1(\lambda_n R)\, e^{\lambda_m \beta\left[1-(1-R^3)^{1/2}\right]} dR \\
C2_{mn} &= \frac{2\lambda_n^2}{\left(\lambda_n^2-1\right)\left(J_1(\lambda_n)\right)^2}\int_0^1 R J_1(\lambda_m R) J_1(\lambda_n R) e^{\lambda_m \beta\left[1-(1-R^3)^{3/2}\right]} dR \\
C3_{mn} &= \frac{2\lambda_n^2}{\left(\lambda_n^2-1\right)\left(J_1(\lambda_n)\right)^2}\int_0^1 \frac{R}{N_{BO}\left(1-R^3+(9/4)\beta^2R^4\right)^{3/2}} \\
&\qquad \times\left\{\left(1-R^3\right)^{1/2}\lambda_m^2 J_1(\lambda_m R) + (9/4)\beta^2R^2(1-R^3)J_1(\lambda_m R) + \right. \\
&\qquad \left.\left[\frac{9\beta^2R^3(1-0.25R^3)(1-R^3)^{1/2}}{\left(1-R^3+(9/4)\beta^2R^4\right)^{1/2}}\right] J_1'(\lambda_m R) J_1(\lambda_n R)\right\} dR
\end{aligned} \tag{31}$$

Solve Equation (30) for a_m

$$a_m = \left[\frac{P_{1n}}{s^2 - \Omega_1^2} + \frac{P_{2n}}{s^2 - \Omega_2^2} + \cdots + \frac{P_{mn}}{s^2 - \Omega_m^2} \right] X_0 \Omega^3 \qquad (\Omega_1^2 < \Omega_2^2 < \cdots < \Omega_m^2) \tag{32}$$

then plug the above solution into Equation (28) and solve it for b_n

$$b_n = \left[\frac{Q_{1n}}{s^2 - \Omega_1^2} + \frac{Q_{2n}}{s^2 - \Omega_2^2} + \cdots + \frac{Q_{mn}}{s^2 - \Omega_m^2} \right] X_0 \Omega^2 \qquad (\Omega_1^2 < \Omega_2^2 < \cdots < \Omega_m^2) \tag{33}$$

The slosh parameters in a low-g environment are

$$\begin{aligned}
w_n &= \Omega_n \sqrt{\frac{a}{R_0}} \\
m_n &= -\left[I_n - \left(\beta - \frac{1}{N_{BO}} \right) \frac{H_n}{\Omega_n^2} \right] (\pi \rho R_0^3) \\
I_n &= \sum_{m=1}^{M} \frac{P_{nm}}{\lambda_m} J_1(\lambda_m) e^{\lambda_m \beta}, \qquad H_n = \sum_{m=1}^{M} Q_{nm} J_1(\lambda_m) \\
h_n &= \left\{ \frac{h}{R_0} - \frac{1}{\Omega_n^2} - \frac{\pi \rho R_0^3}{m_n} \left[\sum_{m=1}^{M} \left(\beta - \frac{1}{\lambda_m} \right) \times \frac{P_{nm} J_1(\lambda_m) e^{\lambda_m \beta}}{\lambda_m} - \beta \left(\beta - \frac{1}{N_{BO}} \right) \frac{H_n}{\Omega_n^2} \right] \right\} R_0
\end{aligned} \tag{34}$$

Notice that the above equation predicts the slosh motions in a cylindrical tank when the liquid height is larger than the tank radius (i.e. $h > R_o$). In the next section, modified slosh model is proposed to extend its application for the case of $h < R_o$.

The high-g smooth wall damping model (Eq. (17)) cannot used to predict slosh damping in a low-g environment. The low-g smooth wall damping of the 1st slosh mass for a circular cylindrical tank has been provided [4]

$$\varsigma_1 = \begin{cases} 0.83 \left(N_{GA} \right)^{-1/2} + 0.096 \left(N_{BO} \right)^{-1/2}, & N_{BO} > 10 \\ 0.83 \left(N_{GA} \right)^{-1/2} \left(1 + 8.2 \left(N_{BO} \right)^{-3/5} \right), & otherwise \end{cases} \tag{35}$$

where the dimensionless parameter Galileo number N_{GA} is defined as

$$N_{GA} = \frac{\Omega_1 R_0^2}{(0.4647)^2 k_\nu} \tag{36}$$

VII. Low-G Slosh Parameters a Cylindrical Tank with h/R_0 Correction

For the case that the height of liquid level is less than the radius of the tank, the slosh parameter models derived by Dodge [3] must be modified as follows [7].

$$\begin{aligned}
w_n &= \Omega_n \sqrt{\frac{a}{R_0}} \sqrt{tanh(\frac{\lambda_n h}{R_0})} \\
m_n &= -\left[I_n - \left(\beta - \frac{1}{N_{BO}} \right) \frac{H_n}{\Omega_n^2} \right] (\pi \rho R_0^3) tanh(\frac{\lambda_n h}{R_0}) \\
h_n &= \left\{ \frac{h}{R_0} - \frac{1}{\Omega_n^2} - \frac{\pi \rho R_0^3}{m_n} \left[\sum_{m=1}^{M} \left(\beta - \frac{1}{\lambda_m} \right) \times \frac{P_{nm} J_1(\lambda_m) e^{\lambda_m \beta}}{\lambda_m} - \beta \left(\beta - \frac{1}{N_{BO}} \right) \frac{H_n}{\Omega_n^2} \right] \right\} R_0 tanh(\frac{\lambda_n h}{2R_0})
\end{aligned} \tag{37}$$

Notice that Equation (37) predicts the slosh motions in the cylindrical tank with a flat bottom. For a cylindrical tank with elliptical top and bottom domes as shown in Figure 4, the tank radius and liquid height in the slosh parameters

must be modified using Equations (19), (20) and (21) for the liquid height in the upper dome, barrel, and lower dome, respectively [7].

The derivation of slosh parameters in Equation (34) assumes that the contact angle is zero based on the linearized approximation [3]. For the 90 degree contact angle case [1], the low-g slosh frequency is

$$w_n^2 = \left[n^2 \lambda_n^2 \frac{\sigma}{\rho R_0^3} + \frac{a}{R_0} \right] \lambda_n \tanh\left(\frac{\lambda_n h}{R_0} \right) \tag{38}$$

If the acceleration a reverses the direction such that $B_o < -(\lambda_1)^2$, then the frequency is imaginary which means the interface will be become unstable. The corresponding critical acceleration

$$a_{crit} = (\lambda_1)^2 \left(\frac{\sigma}{\rho R_0^2} \right) \tag{39}$$

is the minimum adverse acceleration to maintain surface stability under zero-g environment [1].

Unlike Eq. (17), a correction equation involving h/R_0 has not been attempted for low-g slosh damping model (Eq. (35)) due to insufficient data collected [4].

VIII. Mechanical Slosh Toolbox (MST)

All mechanical slosh models derived in the previous sections have been implemented in MATLAB m-functions and are collected in the MST (Mechanical Slosh Toolbox). The assumptions for each model are summarized in the Table 1. The MST can be used to predict slosh dynamics in various body forces (low-g or high-g) by assuming a propellant tank is cylindrical with upper and lower domes. The output of MST are the slosh parameters, which consists of slosh frequency, slosh mass, slosh location and smooth wall slosh damping as functions of liquid fill level, in the mechanical slosh model. Two scripts are provided to help end users to generate slosh parameter data.

- mst_slosh_table.m : generates low-g/high-g slosh tables
- mst_slosh_driver.m : plots low-g/high-g slosh parameters

Model	High G in [1]	Low G in [3]	High G in MST [7]	Low G in MST [7]
Bond Number (Bo)	Bo > 1000	10 < Bo < ∞	Bo > 1000	10 < Bo < ∞
Cylindrical Tank End Dome Assumption	No Domes	No Domes	Rounded Domes	Rounded Domes
Liquid Height Limit	None	$h > R_0$	None	None
Contact Angle	90 degrees	0 degrees	90 degrees	0 degrees
Slosh Parameters	Mass, Frequency, Mass Location, Smooth Wall Damping	Mass, Frequency, Mass Location, Smooth Wall Damping	Mass, Frequency, Mass Location, Smooth Wall Damping	Mass, Frequency, Mass Location, Smooth Wall Damping

Table 1. Assumptions on Mechanical Slosh Models

To demonstrate the uses of the MST, a cylindrical tank with liquid Oxygen propellants filled is assumed. The tank has both elliptical top and bottom domes with arbitrary tank radius of 8.8 feet and dome height of 9.8 feet. For a high-g flight environment, the "mst_slosh_table.m" generates a 1-D lookup table as shown in Figure 6. The lookup variable is LiqLevel. In this example, 20 difference liquid levels are specified between 0.1 ft above the bottom of the tank and 0.1 ft below the top of the tank.

LiqLevel(ft)	Freq(Hz)	Mass(slug)	Zeta(-)	h1(ft)
1.00000e-001	2.95765e-001	4.59062e-001	3.58209e-003	5.00634e-002
2.74285e+000	3.17044e-001	2.96167e+002	2.53919e-004	1.42377e+000
5.38571e+000	3.41341e-001	9.39358e+002	1.54037e-004	2.91349e+000
8.02856e+000	3.68245e-001	1.60573e+003	1.17351e-004	4.53824e+000
1.06714e+001	3.94811e-001	1.96746e+003	1.00994e-004	6.21771e+000
1.33143e+001	4.06851e-001	2.08929e+003	9.44904e-005	7.48280e+000
1.59571e+001	4.10912e-001	2.13121e+003	9.15112e-005	8.30691e+000
1.86000e+001	4.12265e-001	2.14526e+003	8.99413e-005	8.81813e+000
2.12428e+001	4.12713e-001	2.14993e+003	8.78210e-005	9.12568e+000
2.38857e+001	4.12862e-001	2.15148e+003	8.78210e-005	9.30730e+000
2.65285e+001	4.12911e-001	2.15199e+003	8.78210e-005	9.41339e+000
2.91714e+001	4.12927e-001	2.15216e+003	8.78210e-005	9.47496e+000
3.18142e+001	4.12933e-001	2.15222e+003	8.78210e-005	9.51056e+000
3.44571e+001	4.12935e-001	2.15224e+003	8.78210e-005	9.53110e+000
3.70999e+001	4.12935e-001	2.15224e+003	8.78210e-005	9.54293e+000
3.97428e+001	4.12935e-001	2.15225e+003	8.78210e-005	9.54975e+000
4.23856e+001	4.16244e-001	2.05161e+003	8.88786e-005	9.40410e+000
4.50285e+001	4.36733e-001	1.53776e+003	9.55211e-005	8.54553e+000
4.76713e+001	4.95292e-001	7.22800e+002	1.15363e-004	6.64437e+000
5.03142e+001	1.09276e+000	6.26656e+000	3.78063e-004	1.36497e+000

Figure 6. High-g Table from "mst_slosh_table.m"

For a low-g flow flight scenario, the "mst_slosh_table.m" generates a 2-D lookup table as shown in Figure 7. The lookup variables are LiqLevel and Bond Number (or Gravity). In this example, 6 difference liquid levels are specified between 0.1 ft above the bottom of the tank and 0.1 ft below the top of the tank. In addition to the liquid level variable, 6 logarithmically equally spaced Bond numbers are also assigned between decades 10^1 and 10^6 to complete the 2-D lookup variables.

LiqLevel(ft)	1.00000e-001	1.01428e+001	2.01857e+001	3.02285e+001	4.02714e+001	5.03142e+001
Bond Number	1.00000e+001	1.00000e+002	1.00000e+003	1.00000e+004	1.00000e+005	1.00000e+006
Gravity(ft/s^2)	5.28047e-005	5.28047e-004	5.28047e-003	5.28047e-002	5.28047e-001	5.28047e+000
Freq(Hz)						
	3.89616e-004	1.19336e-003	3.76583e-003	1.19414e-002	3.78288e-002	1.19729e-001
	5.14334e-004	1.57536e-003	4.97129e-003	1.57639e-002	4.99379e-002	1.58055e-001
	5.43511e-004	1.66473e-003	5.25331e-003	1.66581e-002	5.27708e-002	1.67021e-001
	5.43959e-004	1.66610e-003	5.25764e-003	1.66719e-002	5.28143e-002	1.67159e-001
	5.43966e-004	1.66612e-003	5.25770e-003	1.66721e-002	5.28150e-002	1.67161e-001
	1.43951e-003	4.40911e-003	1.39136e-002	4.41198e-002	1.39766e-001	4.42363e-001
Mass(slug)						
	5.12120e-001	4.29155e-001	4.41741e-001	4.54312e-001	4.60808e-001	4.63901e-001
	2.14654e+003	1.79879e+003	1.85155e+003	1.90424e+003	1.93147e+003	1.94443e+003
	2.39699e+003	2.00867e+003	2.06758e+003	2.12641e+003	2.15682e+003	2.17130e+003
	2.40094e+003	2.01198e+003	2.07099e+003	2.12992e+003	2.16038e+003	2.17488e+003
	2.40100e+003	2.01203e+003	2.07104e+003	2.12997e+003	2.16043e+003	2.17493e+003
	6.99085e+000	5.85830e+000	6.03012e+000	6.20172e+000	6.29040e+000	6.33262e+000
Zeta(-)						
	3.34844e-002	1.58530e-002	6.55581e-003	2.93673e-003	1.41420e-003	7.20275e-004
	7.77816e-003	1.10525e-002	3.85346e-003	1.41918e-003	5.61566e-004	2.41014e-004
	7.77816e-003	1.10525e-002	3.85346e-003	1.41918e-003	5.61566e-004	2.41014e-004
	7.77816e-003	1.10525e-002	3.85346e-003	1.41918e-003	5.61566e-004	2.41014e-004
	7.77816e-003	1.10525e-002	3.85346e-003	1.41918e-003	5.61566e-004	2.41014e-004
	3.34844e-002	1.58530e-002	6.55581e-003	2.93673e-003	1.41420e-003	7.20275e-004
h1(ft)						
	4.20068e-002	5.05826e-002	5.05170e-002	5.02388e-002	5.01310e-002	5.00913e-002
	4.95198e+000	5.96294e+000	5.95521e+000	5.92242e+000	5.90971e+000	5.90502e+000
	7.56963e+000	9.11499e+000	9.10317e+000	9.05304e+000	9.03361e+000	9.02645e+000
	7.96411e+000	9.59001e+000	9.57757e+000	9.52484e+000	9.50440e+000	9.49686e+000
	8.01374e+000	9.64977e+000	9.63725e+000	9.58419e+000	9.56362e+000	9.55603e+000
	1.14531e+000	1.37913e+000	1.37734e+000	1.36976e+000	1.36682e+000	1.36573e+000

Figure 7. Low-g Table from "mst_slosh_table.m"

The "mst_slosh_driver.m" generates high-g verse low-g comparison plot for the selected tank as shown in Figure 8 where the high-g slosh parameters are plotted in a blue color and the low-g slosh parameters are plotted in a green color.

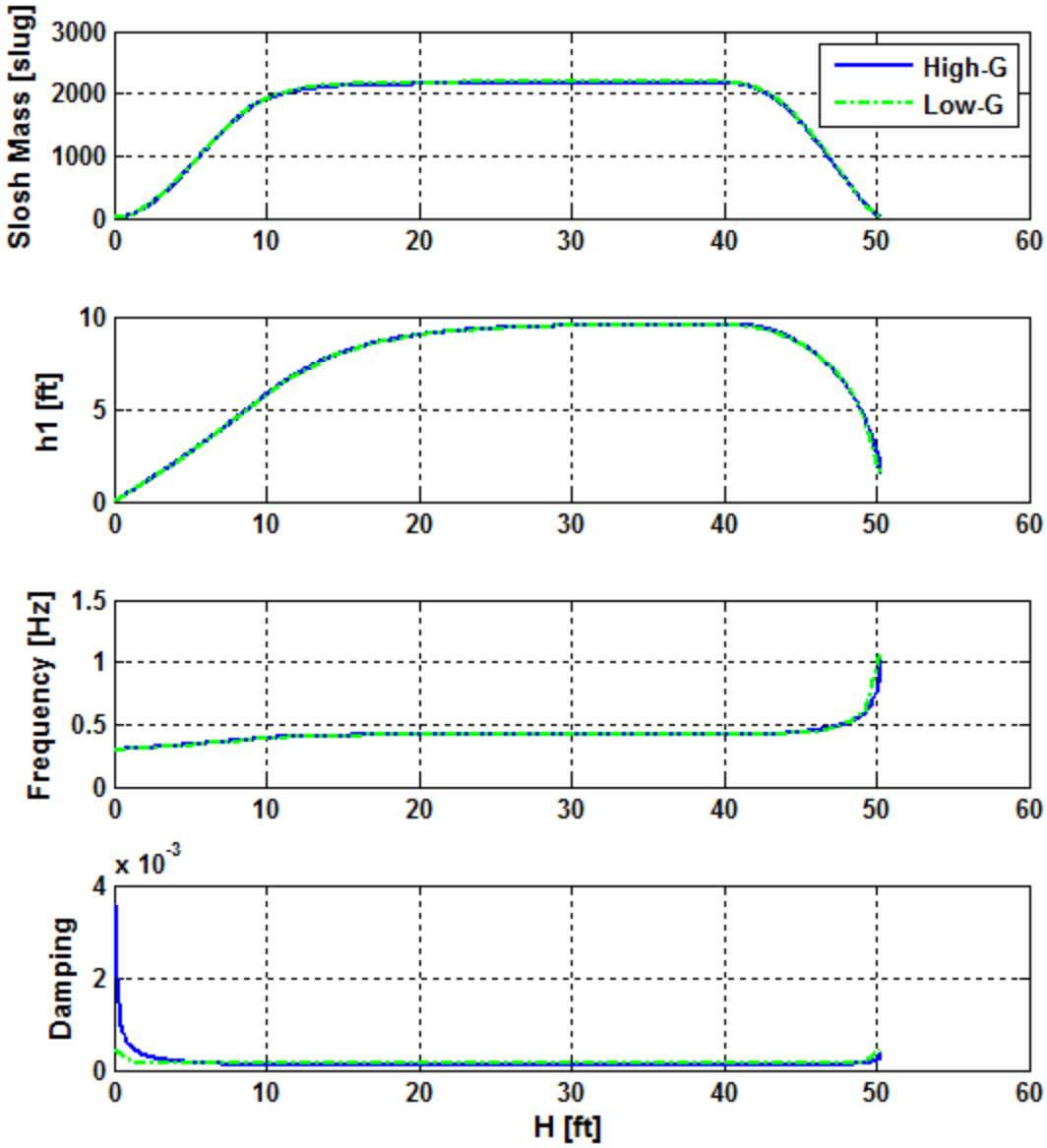

Figure 8. High-g vs Low-g plots "mst_slosh_driver.m"

The high level code flows for both scripts are drawn in Figure 9 and Figure 10. The function list for MST follows.

- any_g_calc.m : Main function used to compute slosh parameters
- low_g_calc.m : Computes slosh parameters using low-G model
- low_g_damp.m : Low-G damping model
- low_g_freq.m : Low-G frequency, mass, and location model (dimensionless)
- fourier_bessel_coeffs.m : Compute Fourier-Bessel coefficients
- bessel_first.m : Bessel function of first kind

- betaFromNbo.m : Solves for beta
- high_g_calc.m : Computes slosh parameters using high-G model
- mst_constants.m : Constants used in the MST

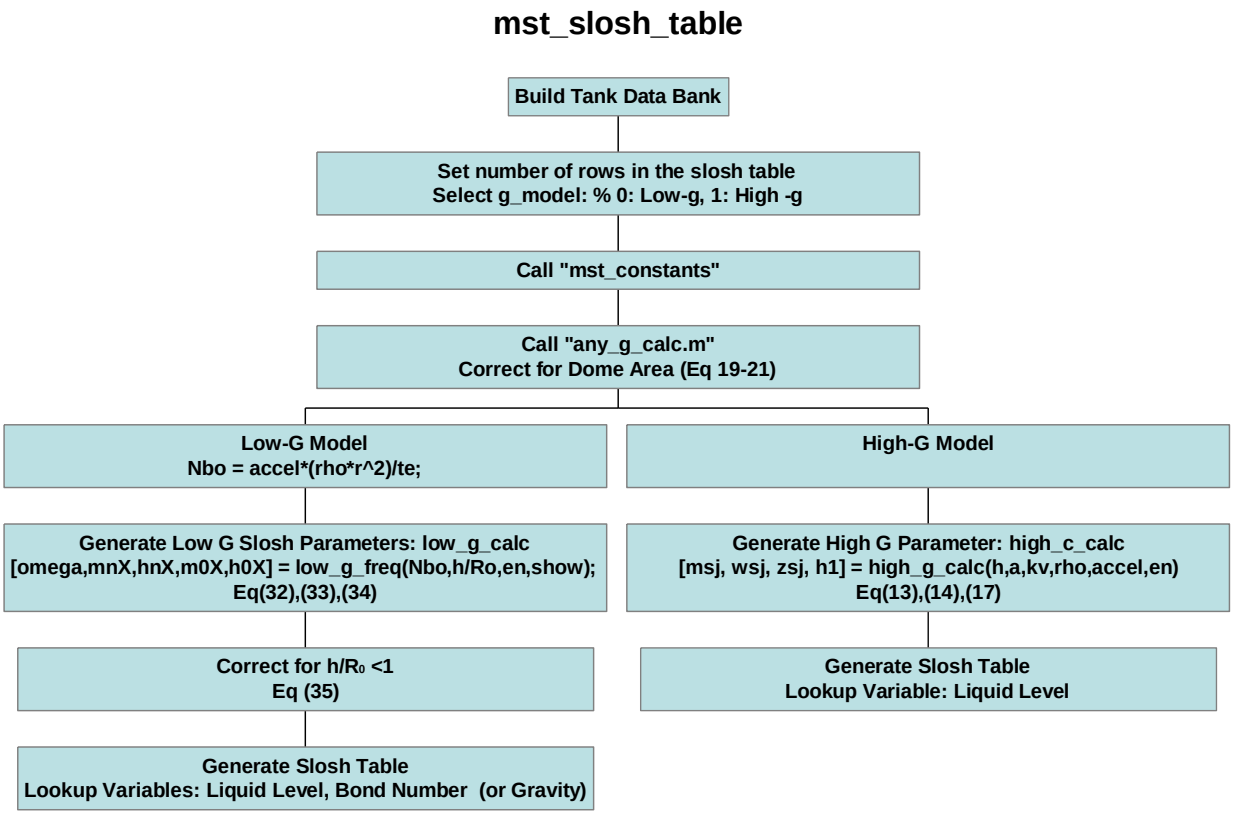

Figure 9. Code Flows for "mst_slosh_table.m"

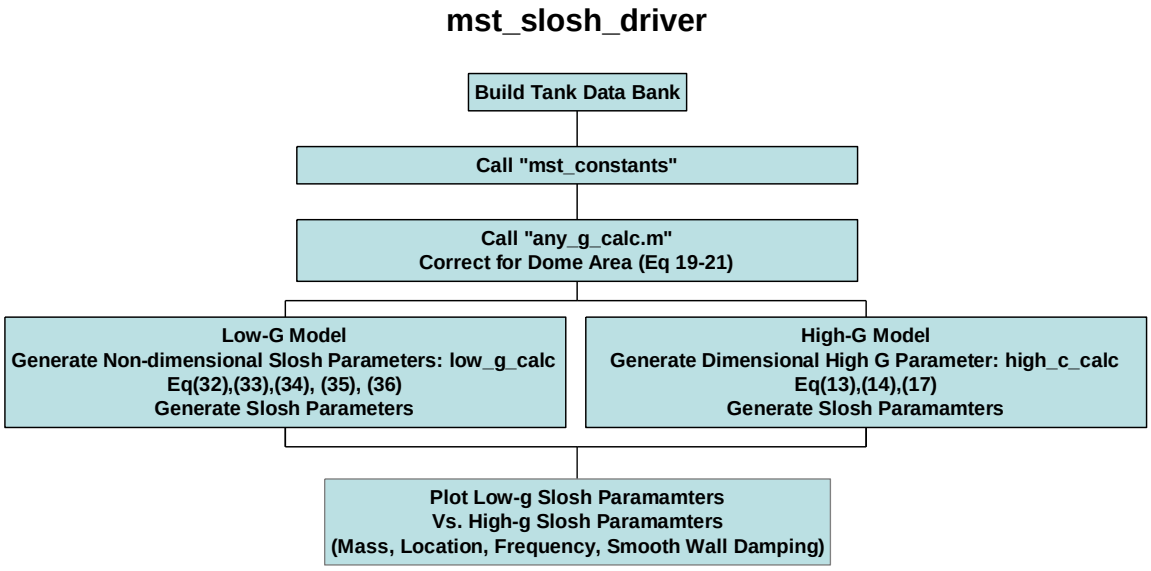

Figure 10. Code Flows for "mst_slosh_driver.m"

IX. Summary

The mechanical slosh models for a cylindrical tank with a flat bottom have been reviewed under this study. The high-g slosh models (Bond number ≥ 1000) from [1] were modified in this study for a cylindrical tank with elliptical domes. For the low Bond number case, the low-g slosh models cited in the literature ([2] to [4]) were also studied. Those low-g models can be used for Bond number > 10; an additional model study may be needed for the smaller Bond number scenario. The low-g slosh models from [2] to [4] were also modified to extend their applications for the case that liquid height is smaller than the tank radius and the case of a cylindrical tank with elliptical domes.

X. References

[1] Dodge, F., "The new "Dynamic Behavior of Liquids in Moving Containers,"" Southwest Research Institute, 2000.

[2] Dodge, F. and Garza, L., "Experimental and Theoretical Studies of Liquid Sloshing at Simulated Low Gravities," Technical Report No. 2, Southwest Research Institute, October 20, 1966.

[3] Dodge, F. and Garza, L., "Experimental and Theoretical Studies of Liquid Sloshing at Simulated Low Gravity," Journal of Applied Mechanics, September 1967, pp. 555-562.

[4] Dodge, F. and Garza, L., "Simulated Low-Gravity Sloshing in Cylindrical Tanks Including Effects of Damping and Small Liquid Depth," Technical Report No. 5, Southwest Research Institute, December 29, 1967.

[5] Frosch, J. A., and Vallely, D. P., "Saturn AS501/S-IC Flight Control System Design," The Journal of Spacecraft, Vol. 4, No. 8, August 1967.

[6] Inman, D. J., *Vibration with Control, Measurement, and Stability*, Prentice Hall, NJ, 1989.

[7] Jang, J.-W., Alaniz, A., "Low-G Slosh Model Study," CSDL Presentation to NASA MSFC EV41 Control Working Group, July 24, 2012.